Ion channel formation by Alzheimer's disease amyloid β-peptide (Aβ40) in unilamellar liposomes is determined by anionic phospholipids

Juan Marcos Alarcón [a], Julio A. Brito [a], Tamara Hermosilla [a], Illani Atwater [a,b], David Mears [a,c,], Eduardo Rojas [a]*

[a] *Institute of Biomedical Sciences, Faculty of Medicine, University of Chile, Independencia 1027, Santiago, Chile*
[b] *J.J. Aguirre Hospital, University of Chile, Santos Dumont 999, Santiago, Chile*
[c] *Department of Anatomy, Physiology and Genetics, Uniformed Services University of the Health Sciences, Bethesda, MD 20814, USA*

A B S T R A C T

Incorporation of Alzheimer's disease amyloid β-proteins (AβPs) across natural and artificial bilayer membranes leads to the formation of cation-selective channels. To study the peptide–membrane interactions involved in channel formation, we used cation reporter dyes to measure AβP-induced influx of Na^+, Ca^{2+}, and K^+ into liposomes formed from phosphatidylserine (PS), phosphatidylinositol (PI) and phosphatidylcholine (PC). We found that Aβ40, but not Aβ40-1 or Aβ28, caused a dose-dependent increase in the concentration of each cation in the lumen of liposomes formed from the acidic phospholipids PS and PI. The Aβ40-induced changes in cation concentration, which we attribute to ion entry through Aβ40 channels, were not observed when using liposomes formed from the neutral phospholipid PC. Using mixtures of phospholipids, the magnitude of the AβP40-induced ion entry increased with the acidic phospholipid content of the liposomes, with entry being observed with as little as 5% PS or PI. Thus, while negatively charged phospholipids are required for formation of cation-permeable channels by Aβ40, a small amount is sufficient to support the process. These results have implications for the mechanisms of AβP cytotoxicity, suggesting that even a small amount of externalized negative charge could render cells susceptible to the deleterious effects of unregulated ion influx through AβP channels.

1.   Introduction

Amyloid β-peptides (AβPs), such as Aβ40 and Aβ42, are constituents of the senile plaques found in various regions of the brain of patients with Alzheimer's disease. These peptides are the products of proteolytic processing of amyloid precursor protein (APP) and have been implicated as causal factors in the neurodegeneration associated with Alzheimer's disease [13,23]. Several lines of evidence indicate that the cytotoxicity of AβPs may be related to a disruption of cellular Ca^{2+} homeostasis subsequent to interaction of the peptide with the plasma membrane [21,33,34,44]. Proposed mechanisms for the AβP-induced Ca^{2+} dysregulation include activation of specific membrane receptors or endogenous Ca^{2+} channels [9,55], disruption of membrane integrity or fluidity [36,38,46], and formation of ion channels by AβPs themselves [5,6,31,37,60].

Numerous works have demonstrated that cytotoxic AβPs can spontaneously incorporate from solution into negatively charged phospholipid bilayers [3,6–8,25,37,41,47,49]. Once in

* *Corresponding author*. Tel.: +56 2 978 6360; fax: +56 2 777 6916.
  E-mail address: dmears@med.uchile.cl (D. Mears).

the membrane, Aβ40 forms Zn^{2+}-sensitive cationic channels with the permeability sequence: $Cs^+ > Li^+ > Ca^{2+} \geq K^+ > Na^+$ [8]. Based on this observation, Arispe et al. proposed that Aβ40 toxicity results from the formation of ion channels in the target membrane, followed by unregulated influx of Na^+ and Ca^{2+}, and efflux of K^+ [5,6]. In support of this concept, Aβ40 was shown to form ion channels in membrane patches from a hypothalamic GnRH neuronal cell line [34] and Aβ40 as well as other cytotoxic peptides can induce a Zn^{2+}-sensitive Ca^{2+} influx in cultured neuronal cells and astrocytes [1,34].

Although the properties of AβP channels and the factors governing their formation have been studied in depth using planar lipid bilayers, less information is available regarding the changes in ion concentration that result from AβP channel activity in three dimensional systems. Unilamellar liposomes, with their large surface area to volume ratio ($\sim 1.5 \times 10^7 \text{ m}^{-1}$), represent an ideal model for such studies. In addition to allowing incorporation of channel-forming proteins, the liposomes can be loaded with compounds, such as fluorescent probes, and have the capacity to generate a membrane potential under conditions of asymmetrical ion distribution [14,17,50,56]. As such, the giant unilamellar liposome is the artificial membrane system that is the nearest to a cellular membrane. Early studies using unilamellar liposomes in conjunction with $^{45}Ca^{2+}$ uptake measurements demonstrated that Aβ40 forms Ca^{2+}-permeable, Zn^{2+}-sensitive channels in liposomes formed from negatively charged phospholipids [42,50].

In this work, we examined the effects of phospholipid composition on Aβ40-induced Na^+, Ca^{2+}, and K^+ entry into giant unilamellar liposomes loaded with fluorescent ion indicators. We found that the peptide stimulated a rapid influx of ions into liposomes containing as little as 5% phosphatidylserine or phosphatidylinositol (acidic), but not into those formed from 100% phosphatidylcholine (neutral). Furthermore, the magnitude of the Aβ40-induced rises in lumenal cation concentration increased steadily with the acidic phospholipid content of the vesicles. These results provide further evidence that membrane insertion and channel formation by Aβ40 is mediated by interactions with negatively changed phospholipids, and support a model, whereby cellular susceptibility to Aβ40 cytotoxicity is determined at least in part by the amount of negative charge on the external leaflet of the plasma membrane.

2. Materials and methods

2.1. Preparation of unilamellar liposomes

Unilamellar liposomes were prepared from mixtures of palmitoyl-oleoyl-phosphatidylserine, palmitoyl-oleoyl-phosphatidylcholine, and palmitoyl-oleoyl-phosphatidylinositol, using a modification of the protocol described by Hope et al. [26,27]. The lipids and were first dissolved in chloroform and mixed in the desired molar ratio. After drying, the lipid mixtures were hydrated for 30 min. The hydration (internal) solution was (in mM): 100, tetramethylammonium hydroxide (TMA); 0.1, ethylene diamine tetraacetic acid (EGTA); 5, tromethamine (Tris); 10, Hepes. The pH of the solution was adjusted to 7.4 with HCl and the osmolarity was adjusted to 190–205 mOsm/l. Finally, 150 µM of the acidic form of the relevant fluorescent probe (SBFI for Na^+; PBFI for K^+; Indo-1 for Ca^{2+}) was added to mixture. The lipid–solution mixture was stirred with a vortex for 1 min and filtered with a 0.1 µm polycarbonate filter. To enhance the unilamellar liposome formation, the mixture was frozen, thawed, and filtered several times.

Following the previous protocol, the preparation was eluted through a Sephadex G-25M column (PD-10, Pharmacia Fine Chemicals, Uppsala, Sweden) in the presence of one of the following external solutions, and collected in 1 ml aliquots using an automatic collector. For liposomes loaded with the Na^+ indicator, SBFI acid, the external solution was (in mM): 100, NaCl; 0.1, EGTA; 10, HEPES. For liposomes loaded with the K^+ indicator, PBFI acid, the external solution was (in mM): 100, KCl; 0.1, EGTA; 10, HEPES acid. Finally, for liposomes loaded with the Ca^{2+} indicator, Indo-1 acid, the external solution was (in mM): 100, TMA-Cl; 1.2, $CaCl_2$; 0.1, EGTA; 10, HEPES acid. The pH of each solution was adjusted to 7.4 and the osmolarity to 190–200 mOsm/l.

2.2. Determination of the phosphate concentration of liposome preparations

We determined the phosphate concentration of each preparation as a measure of the quantity of liposomes. To this end, a 25 µl aliquot of the liposome fraction was incinerated in the presence of 10% $MgNO_3$. The incineration product was then dissolved in a solution of 0.4% ammonia molibdate and 1.25% ascorbic acid in 0.5 M HCl. After incubation for 20 min in a water bath at 45 °C, the absorbance of the samples and of known phosphate standards was measured at 800 nm using a spectrophotometer (Gilford Instruments, Oberlin, OH). Once the total phosphate concentration of the preparations was determined (generally, 0.2–0.3 mM), aliquots were diluted to a final concentration of 55 µM for use in the experiments described below.

2.3. Liposome aggregation studies

Liposome aggregation was monitored by measuring changes in solution absorbance corresponding to increased turbidity [4,39]. PS and PC liposomes were suspended at a final phosphate concentration of 55 µM in the following solution (in mM): 100, NaCl; 0.1, EGTA; 10, HEPES acid (pH 7.4, 200 mOsm/l). The absorbance at 350 nm was then recorded before and after addition of Aβ40.

2.4. Fluorescence measurements

Continuous measurements of fluorescence emission from dye-loaded liposomes were carried out using a modified cuvette-based fluorimeter. The high-sensitivity system was equipped with a UV arc lamp (ORIEL Instruments, Stratford, CT) and a photomultiplier (Products For Research Inc., Danvers, MA) with a high voltage power supply (Thorn Emi, UK). For each experiment, liposomes were dispersed in the relevant external solution to a final phosphate concentration of 55 µM and placed in a 10 mm quartz cuvette that was then

loaded into the fluorimeter chamber. The dye in the liposomes was excited at 350 nm for SBFI and PBFI, and at 340 nm for Indo-1. The fluorescence emission was measured at 505 nm (SBFI and PBFI) or 405 nm (Indo-1). During the experiments, the photomultiplier signal was recorded on videotape (Unitrade, Toshiba, Japan) and digitized to a PC using a DMA TL-1 interface and Axoscope software (Axon Instruments, Foster City, CA). Finally, we used Origin 6.1 software (OriginLab Inc., Northampton, MA) to filter the signals by adjacent averaging and to prepare figures. Each experiment lasted 5 min or less, during which no bleaching of the fluorescence signal was noted.

2.5. Calibration curves

Because the background fluorescence of the liposome preparations was variable, the data in this paper are presented as uncalibrated measurements of fluorescence intensity at the emission wavelengths of the reporter dyes, with the background level manually set to zero at the start of each experiment. However, in order to estimate the detection range of our system, we constructed empirical calibration curves for each probe. We first estimated the total amount of probe inside the liposomes within the cuvette. Using a ratio of liposome volume to phospholipid concentration of 2.2 μl/μmol, from Hope et al. [26,27], we calculated a volume of 0.24 μl for the 55 μM of phosphate used for these experiments. The total amount of dye was then calculated as 36 pmol. The calibration curves were obtained by adding increasing amounts of the corresponding cation to solutions containing the calculated amount of probe (Fig. 1). The relationship between the ion concentration and the probe emission was fit with a sigmoidal equation, with half-maximal emission concentrations of 3.4 mM for Na^+ (SBFI), 0.6 μM for Ca^{2+} (Indo-1), and 3.6 mM for K^+ (PBFI).
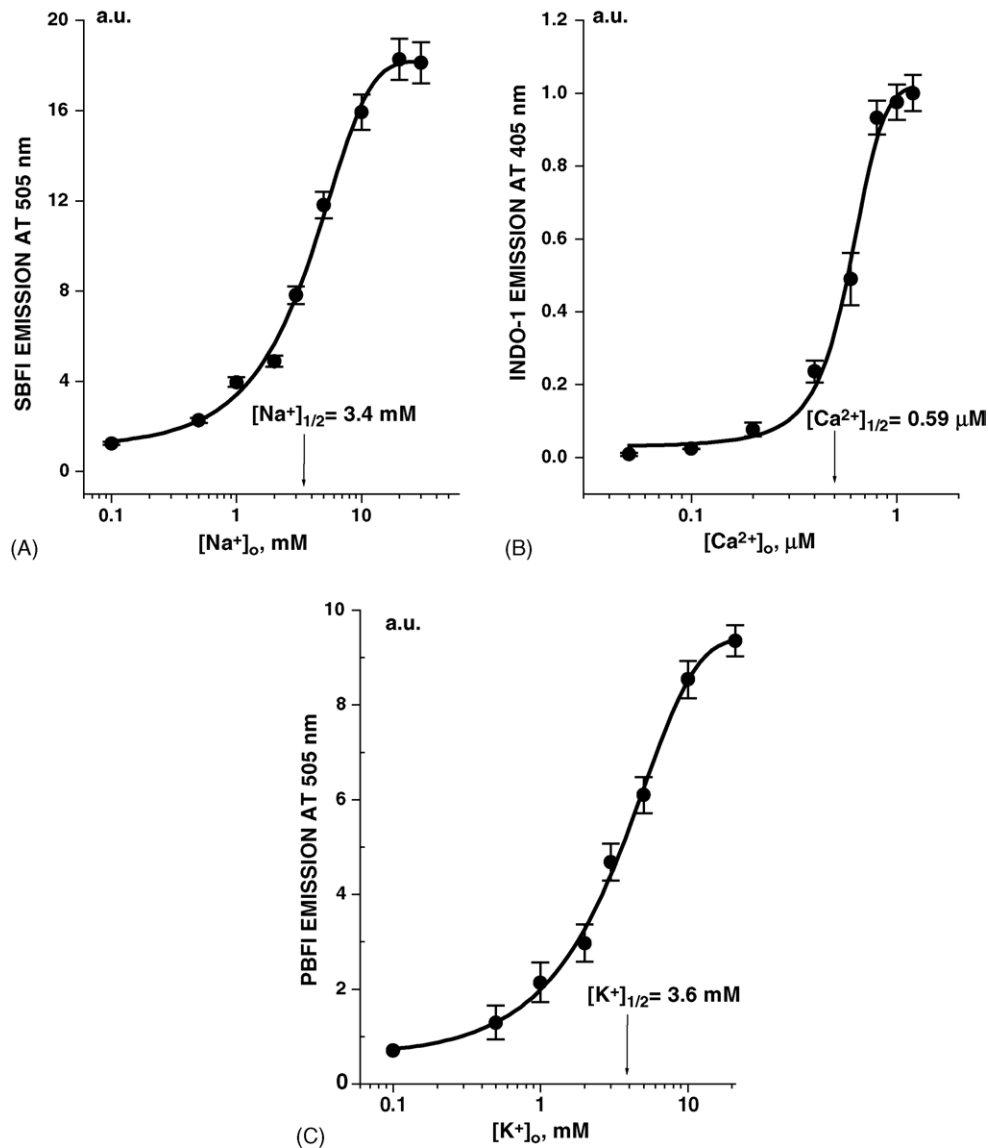

Fig. 1 – In vitro calibration curves for: (A) SBFI (Na^+); (B) Indo-1 (Ca^{2+}); (C) PBFI (K^+). Each curve was obtained by adding increasing concentrations of the respective ion to a 100 mM TMA-Cl buffer solution and measuring the steady-state dye emission at the indicated wavelengths. The values in each curve are mean $\pm$ the standard error (*n* = 4).

2.6. Drugs and peptides

Lipids were purchased from Avanti Polar Lipids Inc. (Alabaster, AL). The synthetic peptides used in this work (Aβ40, Aβ40-1, Aβ28) were all from Bachem (Torrance, CA). The purity of each peptide batch was certified as >99% by HPLC analysis. The acid form of the fluorescent probes SBFI, PBFI, and Indo-1 were obtained from Molecular Probes (Eugene, OR). All other reagents were from Sigma (St. Louis, MO) and Calbiochem (San Diego, CA).

2.7. Presentation of data and statistics

Data are presented as mean ± S.E.M. Curve fitting was performed using Origin 6.1 software. Each time course of fluorescence emission presented in the figures is representative of four to six repetitions of the experiment. Statistical analysis was performed using paired and unpaired Student's t-tests.

3. Results

3.1. Aβ40 evokes dose-dependent Na^+ and Ca^{2+} entry in PS liposomes

Fig. 2A shows the time course of 505 nm fluorescence emission measured from freely suspended PS liposomes loaded with the Na^+ reporter dye SBFI. Application of Aβ40 induced a rapid elevation of the emission at 505 nm, which reached a plateau within several seconds. The steady-state emission reached progressively higher levels as the concentration of the peptide was increased from 1 to 10 μM. To confirm that the system detects changes in the lumenal free Na^+ concentration, a separate set of SBFI-loaded liposomes was exposed to the Na^+-specific exchanger monensin. As expected, monensin induced a rapid increase in the 505 nm emission from the SBFI trapped within the vesicles (Fig. 2A, inset). As shown in Fig. 2B, Aβ40 also evoked a dose-dependent increase in the 405 nm fluorescence emission when applied to vesicles loaded with the Ca^{2+} indicator Indo-1. In this case, the functionality of the system was confirmed by measuring the response of Indo-1-loaded liposomes to the Ca^{2+} ionophore, A23187 (Fig. 2B, inset). The Aβ40-induced rises in both Na^+ and Ca^{2+} concentration were attenuated by approximately 50% in the presence of 100 μM Zn^{2+} (data not shown), an antagonist of AβP channels [7,32,34,42].

Fig. 3 is a dose–response curve for the Aβ40-evoked increase in Indo-1 fluorescence emission from liposomes formed by PS. The relationship between steady-state dye emission and Aβ40 concentration was non-linear over the range tested, and could be fit by a Boltzmann function with a half-maximal Aβ40 concentration of 3.3 μM. Together, the data in Figs. 2 and 3 indicate that Aβ40 is able to induce entry of the cations Na^+ and Ca^{2+} from the external medium.

Recent data have demonstrated that AβPs can induce aggregation of liposomes, the rate of which depends on membrane lipid composition and other experimental conditions [4,39,40]. Since the increase in solution turbidity caused by liposome aggregation is associated with increased light
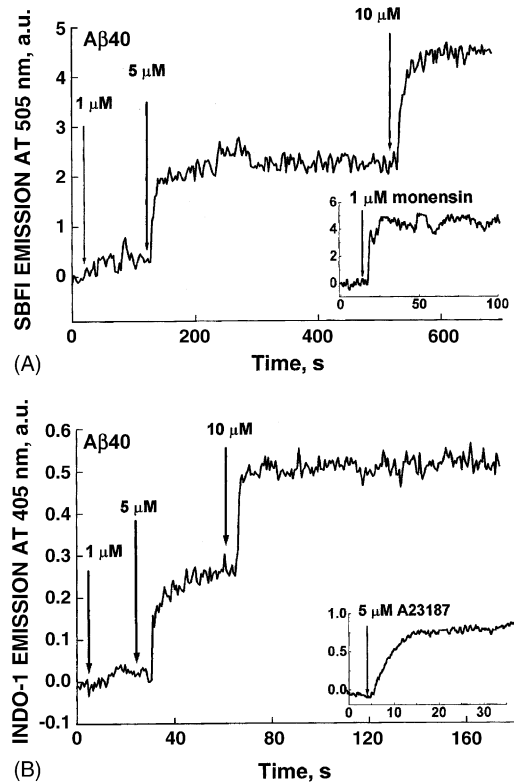

Fig. 2 – Aβ40-induced Ca^{2+} and Na^+ entry in unilamellar liposomes. (A) Addition of increasing concentrations of Aβ40 induced an increase of the fluorescence emission from the Na^+ indicator SBFI. The inset shows the increase in SBFI emission evoked by 1 μM monensin. (B) Addition of increasing concentrations of Aβ40 induced an increase in emission from the Ca^{2+}-sensitive dye Indo-1. The inset shows the emission increase evoked by 5 μM A33187. Each curve is representative of six experiments.
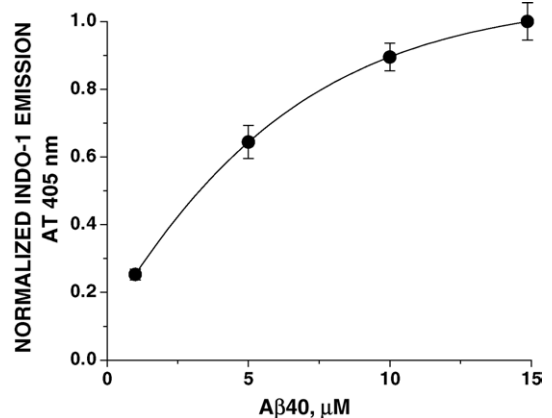

Fig. 3 – Concentration dependence of Aβ40-induced Ca^{2+} entry in PS liposomes. Liposomes made from PS were loaded with Indo-1 and exposed to various concentrations of Aβ40, and the increase in fluorescence emission from the dye was recorded. The data were normalized to the change in emission induced by 15 μM Aβ40 and fit with a Boltzmann function. Points represent mean ± S.E.M. (n = 4–5).

absorbance, liposome aggregation could conceivably attenuate the signal emitted from the fluorescent probes. Such attenuation would not affect our conclusion that Aβ40 induces cation entry in PS liposomes, but could result in an underestimate of the magnitude of the effect. However, using liposomes without reporter dyes, under the conditions and time frame of our experiments, we observed that Aβ40 did not produce the increase in absorption at 350 nm that is characteristic of liposome aggregation (data not shown). We, therefore, concluded that our experimental results are not affected by Aβ40-induced liposome aggregation.

3.2. Aβ40-1 and Aβ28 do not induce ion influx across unilamellar liposomes formed from PS

As shown in Fig. 4, Aβ40 evoked an increase of the SBFI, Indo-1, or PBFI emission, representative of entry of the respective cation, but this effect was not observed, when either the reverse sequence of the peptide, Aβ40-1, or a truncated form of the peptide, Aβ28, was used. The same results were observed when the addition sequence was changed (i.e., Aβ40-1, then Aβ28, then Aβ40, changed to Aβ28, then Aβ40-1, then Aβ40, etc.), eliminating the possibility of any cumulative influence of one type of peptide on the others (data not shown). Aβ40-1, despite having the same amino acid sequence, has a different spatial structure compared to the cytotoxic Aβ40. On the other hand, Aβ28 lacks the hydrophobic C-terminal of Aβ40, which corresponds to the transmembrane α-helix region of APP and

is likely the site of insertion of Aβ40 into lipid membranes [29]. The results in Fig. 4 indicate that these structural differences result in an inability of Aβ40-1 and Aβ28 to form cation-permeable channels in liposomes formed from PS.

3.3. Aβ40, Aβ40-1, and Aβ28 do not induce ion influx in unilamellar liposomes formed from phosphatidylcholine

The observation that Aβ40 preferentially forms ion channels in negatively charged lipid bilayers [6,25,54] raises the question of whether Aβ40 can incorporate into liposomes formed from neutral phospholipids and induce ion influx. Fig. 5 shows that Aβ40-1, Aβ28, and most notably, Aβ40, did not change the SBFI, Indo-1, or PBFI emission when they were added to liposomes formed from PC. At the end of each experiment, the functionality of the fluorescent probe in the liposomes was demonstrated using the corresponding Na^+, Ca^{2+} or K^+ ionophores. These results demonstrate that Aβ40 does not form channels in liposomes formed from neutral phospholipids.

We next examined the ability of Aβ40 to form channels in liposomes formed from mixtures of PS and PC. The superimposed records in Fig. 6A show that 5 μM Aβ40 induced a larger elevation of the Indo-1 fluorescence emission from liposomes composed of 50% PS than from those containing 5% PS. The difference in response between the two populations of liposomes did not result from differences in the quantity of liposomes or the extent of loading with the indicator, since the
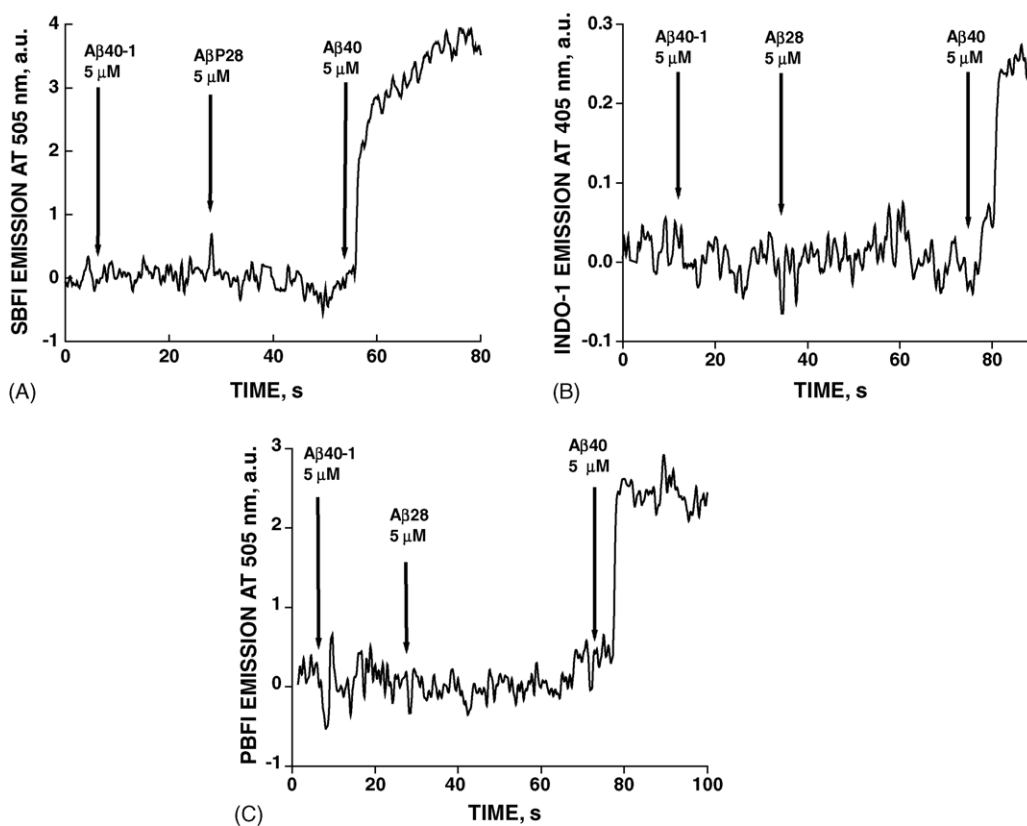

Fig. 4 – Effects of different AβPs on ion entry in PS liposomes. Liposomes formed from PS were loaded with: (A) the Na^+ indicator SBFI; (B) the Ca^{2+} indicator Indo-1; (C) the K^+ indicator PBFI, and were exposed to Aβ40-1, Aβ28 and Aβ40 as indicated by the arrows. The data are representative of five experiments with each indicator.
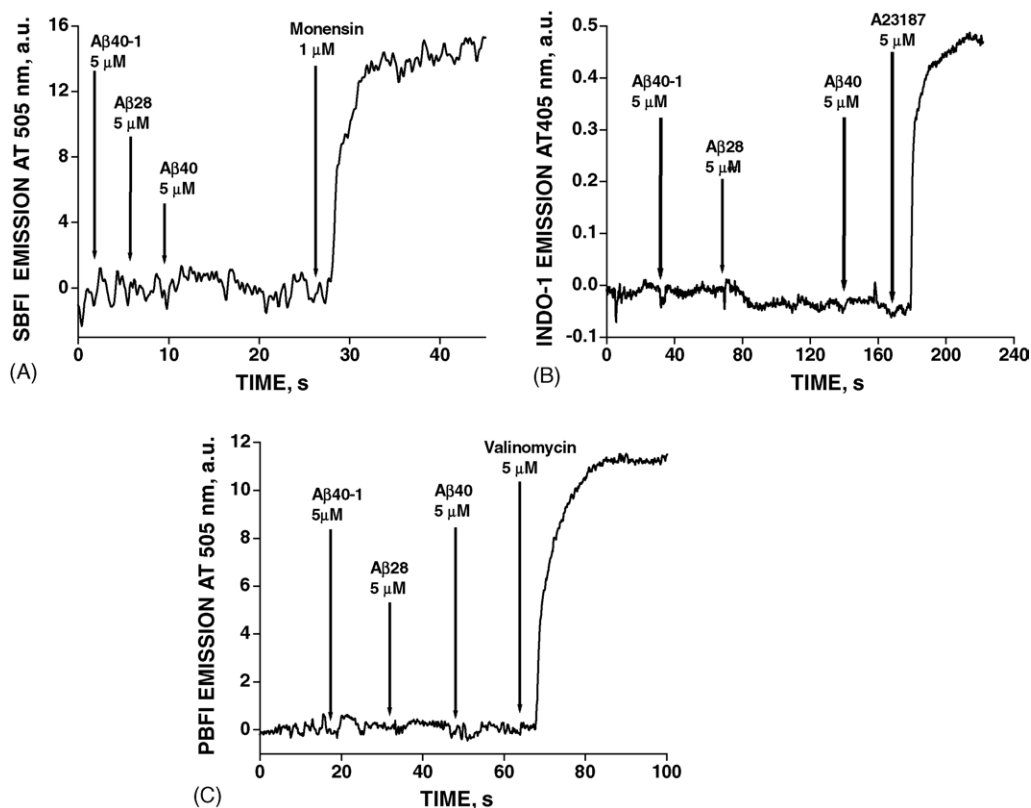
Fig. 5 – Amyloid peptides do not induce ion entry in PC liposomes. Liposomes formed from PC were loaded with: (A) the Na$^+$ indicator SBFI; (B) the Ca^{2+} indicator Indo-1; (C) the K$^+$ indicator PBFI and were exposed to Aβ40-1, Aβ28 and Aβ40 as indicated by the arrows. The peptides produced no change in lumenal cation concentrations, whereas the Na$^+$ exchanger monensin (A); the Ca^{2+} ionophore A23187 (B); the K$^+$ ionophore valinomycin (C)-induced rapid increases in the emission of the respective ion-sensitive dyes. The data are representative of five experiments with each indicator.

Indo-1 emission reached the same plateau upon addition of the Ca^{2+} ionophore A23187 at the end of each experiment. As shown in Fig. 6B, the steady-state, Aβ40-induced increase in Indo-1 fluorescence emission increased steadily with the PS content of the liposomes. Interestingly, the presence of as little as 5% PS in the liposomes was sufficient to observe a small but significant Ca^{2+} entry in response to Aβ40 ($p < 0.01$). The data were fit with a Boltzmann function with half-maximal response occurring at a PS content of 24%.

We next sought to determine if the facilitation of Aβ40-induced ion influx observed in liposomes with increasing acidic phospholipid content is specific for PS. To this end, we performed experiments using a different acidic phospholipid, phosphatidylinositol (PI), also in mixtures with PC. Fig. 7 shows that Aβ40 did indeed induce a rise in the lumenal-free Ca^{2+} concentration of liposomes containing as little as 5% PI. Similar to the experiments with PS, the steady-state increase in Ca^{2+} concentration was greater in liposomes composed of 50% PI compared to 5% PI ($p < 0.03$, $n = 4$). No rise in the Ca^{2+} concentration was observed when liposomes formed from PI were exposed to Aβ40-1 or Aβ28 (data not shown). Together, the results demonstrate that the capacity of Aβ40 to induce ion influx in unilamellar liposomes is determined by the amount, and not the specific type of acidic phospholipid in the membrane.

4. Discussion

4.1. Aβ40 induces ion influx in unilamellar liposomes

The central premise of the ion channel hypothesis for Alzheimer's disease is that wayward cation flux through channels formed by amyloid β-peptides (AβPs) in neuronal membranes disrupts intracellular ion homeostasis, resulting in cellular dysfunction and death [5,6,32]. In support of this theory, AβPs have been shown to form channels in cell membranes [22,34,51] and also to alter the intracellular Ca^{2+} concentration in some cells [21,35,44]. However, to date, it has been difficult to draw a causal link between the two phenomena, owing in part to the complexity of the mechanisms involved in regulating intracellular ion concentrations. Studies of the magnitude and kinetics of AβP-induced changes in ion concentration in model systems will likely aid such efforts, by providing a basis for predicting and interpreting the effects of the peptides in vivo. In this study, we describe results with giant unilamellar liposomes loaded with fluorescent reporter dyes, a system that allows the monitoring of lumenal cation concentrations with high time resolution.

We report here that Aβ40 induces a rapid increase in the concentration of free Na$^+$, Ca^{2+}, and K$^+$ in the lumen of liposomes formed by PS and PI. We attribute these concentra-
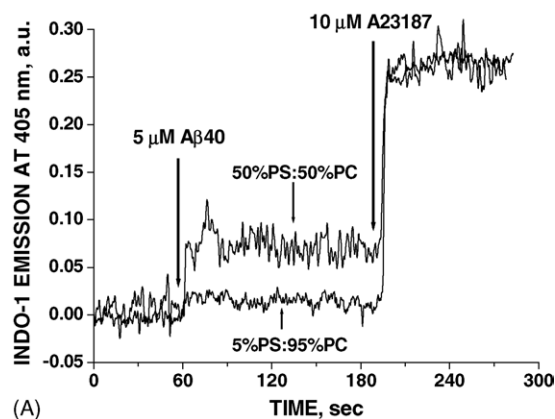
(A)
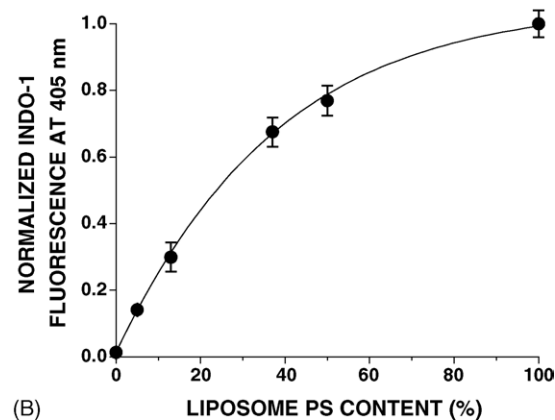
(B)

Fig. 6 – Effect of phospholipid composition on Aβ40-induced Ca²⁺ entry into unilamellar liposomes. (A) Superimposed recordings of Aβ40-stimulated changes in Indo-1 fluorescence measured from liposomes formed from 50% PS:50% PC or 5% PS:95% PC. The Ca²⁺ ionophore A23187 increased the Indo-1 emission similarly in both preparations. The data are representative of four experiments with each phospholipid combination. (B) The steady-state increase in Indo-1 fluorescence emission induced by 5 μM Aβ40 in PS:PC liposomes is plotted as a function of the PS content. Points represent mean ± S.E.M. for four observations. The data were fit with a Boltzmann function.

Fig. 7 – Aβ40 induces Ca²⁺ entry into liposomes containing phosphatidylinositol (PI). Superimposed recordings of Aβ40-stimulated changes in Indo-1 fluorescence measured from liposomes composed of 50% PI:50% PC or 5% PI:95% PC. The Ca²⁺ ionophore A23187 increased the Indo-1 emission similarly in both preparations. The data are representative of four experiments with each phospholipid combination.

tion increases to influx of the respective cations following incorporation of Aβ40 into the vesicle membrane and formation of cation-permeable channels, as has been described using planar lipid bilayers [3,6,8,37]. Indeed, when using peptide sequences that lack the necessary structural elements to form channels in lipid membranes, such as Aβ40-1 and Aβ28, no changes in lumenal cation concentrations were observed. That channel formation mediates the effects of Aβ40 on lumenal ion concentrations is further supported by the ability of Zn²⁺ to attenuate the response at concentrations known to partially inhibit Aβ40 channels [7,42].

4.2. Concentration dependence of Aβ40-induced ion influx

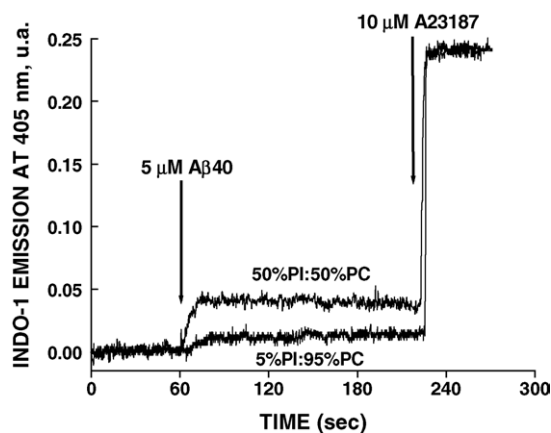The Aβ40-induced increase in dye emission was concentration-dependent, rising rapidly to a higher plateau after each

addition of the peptide. We interpret the dose dependence to reflect an increase in the number of liposomes containing at least one functional Aβ40 channel at higher peptide concentrations. This is suggested by the expectation that even a single functional Aβ40 channel in the membrane of a liposome is expected to cause the lumenal concentration of permeant ions to equilibrate with external levels, after which the formation of new channels would not affect ion flux. At first glance, based on estimations of the molar ratio of Aβ40 to liposomes in our experiments, it would seem unlikely that a portion of the liposomes would be spared from channel formation. Thus, assuming a mean liposome diameter of 100 nm and our estimate of 0.24 μl for the total liposome volume in the cuvette, even at 1 μM Aβ40 the peptide molecules would outnumber the liposomes by 3 or 4 orders of magnitude. However, it is possible that a large percentage of the Aβ40 molecules present were not in the proper conformation or oligomeric form for channel insertion. Furthermore, the exact stoichiometry of Aβ40 channels is not known, nor is the percentage of insertions that result in formation of a functional channel. Thus, it is feasible that less than 100% of the liposomes were affected by Aβ40 channel formation in our experiments. In fact, our results are in accord with the observation of McLaurin and Chakrabartty [46], that AβPs in molar excess can interact strongly with a limited number of liposomes while leaving others untouched.

In contrast, by measuring ⁴⁵Ca²⁺ uptake in unilamellar liposomes reconstituted with Aβ40, Lin et al. showed that tracer content in the liposomes after 30 min was nearly equal to the amount expected if Ca²⁺ had reached equilibrium with the external solution in 100% of the vesicles [42]. The difference between those results and the data presented here is probably related to he experimental methods employed. Thus, Lin et al. used a higher concentration of Aβ40 (~100 μM), and reconstituted the peptide directly into the liposomes

during preparation of the vesicles. This design likely resulted in a higher probability that at least one functional channel would form in each liposome, such that the Ca^{2+} concentration would equilibrate across the membrane during the 30 min observation period.

4.3. *Aβ40-induced ion influx depends on acidic phospholipids*

We also found that stimulation of cation influx by Aβ40 required that the liposomes be composed of at least a small amount of acid phospholipid. This result is in accord with previous studies in planar lipid bilayers, which have demonstrated preferential formation of Aβ40 channels in negatively charged membranes [6,7,25]. In addition, studies using a variety of approaches, including measurements of liposome aggregation [39,40,45], amyloid fibril formation [10,16,58], and AβP membrane insertion [30,53], have also led to the conclusion that the peptides interact specifically with acidic phospholipids. The affinity of AβPs for acidic phospholipids is most likely based on electrostatic interactions, as the effects of the peptides are attenuated when surface charge is reduced by varying salt concentrations or pH [20,43,45]. A similar result is observed with charge screening agents, such as phloretin and annexin 5 [24,40]. Our data showing that Aβ40 induces ion influx in liposomes formed from either PS or PI agree with other studies showing that AβPs can interact with acidic phospholipids having vastly different head group structure [16,45,58]. Together, these data support the concept that electrostatic rather than structural interactions govern the affinity of AβPs for acidic phospholipids.

Recent studies indicate that membrane fluidity affects AβP incorporation into natural and artificial membranes. Thus, cholesterol, which potently decreases membrane fluidity, has been shown to inhibit Aβ40-induced Ca^{2+} elevations in a neuronal cell line [35], aggregation of PS liposomes [4,52], and channel formation by AβPs in planar lipid bilayers [43]. In preliminary studies, we have also found that the Ca^{2+} rise induced by Aβ40 in PS liposomes is ablated by adding cholesterol to the membrane (unpublished results). Nevertheless, changes in membrane fluidity did not likely mediate the effects phospholipid content on Aβ40-induced ion influx described here. This is because the fluidity of cholesterol-free membranes is mainly determined by the length and degree of saturation of the phospholipids, which were kept constant in our experiments [28]. Although the polar head of the phospholipids can also influence membrane fluidity, the effects are most closely related to head size, which is similar for PS and PC [12,48].

The inability of Aβ40 to form channels in neutral phospholipid membranes probably reflects a lack of insertion of the peptide into the membrane, rather than an inability to form a functional channel once incorporated. Thus, our previous study using planar lipid bilayers showed that the charge displacement associated with incorporation of Aβ40 into the bilayer did not occur when the membrane was formed by PC [54]. Circular dichroism analysis also indicates that the extent of Aβ40 incorporation into lipid bilayers increases with the content of acidic phospholipids [53]. The structural basis

for this behavior has been studied by Ji et al. [29], who showed that interaction with PC causes Aβ40 to adopt a mostly β-sheet structure, thereby losing the α-helix structure that is associated with peptide insertion [18,29]. On the other hand, acidic phospholipids not only allow Aβ40 to adopt a structure conducive to insertion of the peptide, but may also serve to electrostatically anchor the peptide in the membrane by interacting with the positively charged Lys28 residue of Aβ40 [10].

4.4. *Implications for AβP-mediated cytotoxicity*

Although these experiments were performed in an artificial membrane system, we believe the work is relevant to understanding the pathophysiology of amyloid-based diseases. In particular, our results suggest that cellular susceptibility to unregulated ion influx through AβP channels, and hence AβP toxicity, should depend in part on the acidic phospholipid content of the membrane. This is consistent with evidence indicating that the toxic effects of AβPs result from their interaction with acidic phospholipids [24,40].

Normally, negatively charged phospholipids, particularly PS, are maintained on the inner leaflet of the cell membrane by energy-dependent mechanisms [19]. Lee et al. have, therefore, proposed that AβPs selectively attack metabolically compromised or pre-apoptotic cells, with externalized PS acting as an electrostatic 'receptor' for AβPs to bind and exert toxic effects [40]. Our demonstration that Aβ40 stimulates cation influx in liposomes formed from as little as 5% PS indicates that even small perturbations in the phospholipid distribution of the plasma membrane could result in AβP-mediated disruption of intracellular ion homeostasis. While this 'metabolic stress' hypothesis requires further experimental verification, recent evidence supports a relationship between cellular energy state and AβP cytotoxicity. In hippocampal neurons, increasing cellular energy production resulted in an attenuation of the cytotoxicity of Aβ25–35 [11], whereas metabolic inhibition had the opposite effect [2]. Furthermore, human teratocarcinoma cybrid cells expressing mitochondrial DNA (mtDNA) from Alzheimer's patients had lower ATP levels and were more sensitive to Aβ40-induced apoptosis than cybrids expressing mtDNA from control subjects [15]. Future tests of this hypothesis should examine the relationship between cellular energy levels and the capacity of AβP to alter intracellular ion concentrations.

Finally, it warrants mention that in addition to surface charge, membrane fluidity is also an important determinant of cellular susceptibility to AβP toxicity. Increasing membrane fluidity by lowering the cholesterol content is associated with enhanced AβP cytotoxicity, while lowering fluidity by increasing cholesterol has a protective effect [4,52,57,59]. The relative importance of fluidity versus surface charge for the interaction of AβPs with natural membranes in vivo remains to be determined. However, in cells the two mechanisms may not be completely independent. Thus, Arispe and Doh have suggested that in PC12 cells, decreasing membrane cholesterol is associated with an increase in the PS level in the external leaflet [4], which could contribute to the enhanced Aβ40 toxicity observed under conditions of reduced membrane cholesterol content.

5. Conclusions

In summary, this work demonstrates the utility of the unilamellar liposome system in conjunction with cation-sensitive probes for studying the properties of ion fluxes resulting from the interaction of AβPs with lipid membranes. We extend previous work in the field by showing that the ability of AβP40 to stimulate Na^+, Ca^{2+}, and K^+ influx is determined by the content of acidic phospholipids in the membrane. These data provide further experimental support for the ''ion channel hypothesis'', first developed by Arispe et al. to explain the neurotoxicity of Aβ40 in the central nervous system [5,6].

Acknowledgements

REFERENCES

[1] Abramov AY, Canevari L, Duchen MR. Changes in intracellular calcium and glutathione in astrocytes as the primary mechanism of amyloid neurotoxicity. J Neurosci 2003;23:5088–95.

[2] Arias C, Montiel T, Quiroz-Baez R, Massieu L. Beta-amyloid neurotoxicity is exacerbated during glycolysis inhibition and mitochondrial impairment in the rat hippocampus in vivo and in isolated nerve terminals: implications for Alzheimer's disease. Exp Neurol 2002;176:163–74.

[3] Arispe N. Architecture of the alzheimer's AbP ion channel pore. J Membr Biol 2004;197:33–48.

[4] Arispe N, Doh M. Plasma membrane cholesterol controls the cytotoxicity of alzheimer's disease AbP (1–40) and (1–42) peptides. FASEB J 2002;16:1526–36.

[5] Arispe N, Pollard HB, Rojas E. Beta-amyloid Ca^{2+}-channel hypothesis for neuronal death in Alzheimer disease. Mol Cell Biochem 1994;140:119–25.

[6] Arispe N, Pollard HB, Rojas E. Giant multilevel cation channels formed by alzheimer disease amyloid beta-protein [AbP-(1–40)] in bilayer membranes. Proc Natl Acad Sci USA 1993;90:10573–7.

[7] Arispe N, Pollard HB, Rojas E. Zn^{2+} interaction with Alzheimer amyloid β protein calcium channels. Proc Natl Acad Sci USA 1996;93:1710–5.

[8] Arispe N, Rojas E, Pollard HB. Alzheimer disease amyloid β protein forms calcium channels in bilayer membranes: blockade by tromethamine and aluminum. Proc Natl Acad Sci USA 1993;90:567–71.

[9] Blanchard BJ, Thomas VL, Ingram VM. Mechanism of membrane depolarization caused by the Alzheimer Ab1–42 peptide. Biochem Biophys Res Commun 2002;293:1197–203.

[10] Bokvist M, Lindstrom F, Watts A, Grobner G. Two types of Alzheimer's β-amyloid (1–40) peptide–membrane interactions: aggregation preventing transmembrane anchoring versus accelerated surface fibril formation. J Mol Biol 2004;335:1039–49.

[11] Brewer GJ, Wallimann TW. Protective effect of the energy precursor creatine against toxicity of glutamate and β-amyloid in rat hippocampal neurons. J Neurochem 2000;74:1968–78.

[12] Browning JL. Motions and interactions of phospholipid head groups at the membrane surface. Part 3: dynamic properties of amine-containing head groups. Biochemistry 1981;20:7144–51.

[13] Butterfield DA, Boyd-Kimball D. Amyloid β-peptide(1–42) contributes to the oxidative stress and neurodegeneration found in Alzheimer disease brain. Brain Pathol 2004; 14:426–32.

[14] Calissano P, Alema S, Fasella P. Interaction of s-100 protein with cations and liposomes. Biochemistry 1974;13:4553–60.

[15] Cardoso SM, Santana I, Swerdlow RH, Oliveira CR. Mitochondria dysfunction of Alzheimer's disease cybrids enhances Ab toxicity. J Neurochem 2004;89:1417–26.

[16] Chauhan A, Ray I, Chauhan VP. Interaction of amyloid β-protein with anionic phospholipids: possible involvement of lys28 and c-terminus aliphatic amino acids. Neurochem Res 2000;25:423–9.

[17] Clement NR, Gould JM. Pyranine (8-hydroxy-1,3,6-pyrenetrisulfonate) as a probe of internal aqueous hydrogen ion concentration in phospholipid vesicles. Biochemistry 1981;20:1534–8.

[18] Curtain CC, Ali FE, Smith DG, Bush AI, Masters CL, Barnham KJ. Metal ions, pH, and cholesterol regulate the interactions of Alzheimer's disease amyloid-β peptide with membrane lipid. J Biol Chem 2003;278:2977–82.

[19] Daleke DL. Regulation of transbilayer plasma membrane phospholipid asymmetry. J Lipid Res 2003;44:233–42.

[20] Del Mar Martinez-Senac M, Villalain J, Gomez-Fernandez JC. Structure of the Alzheimer β-amyloid peptide (25–35) and its interaction with negatively charged phospholipid vesicles. Eur J Biochem 1999;265:744–53.

[21] Demuro A, Mina E, Kayed R, Milton SC, Parker I, Glabe CG. Calcium dysregulation and membrane disruption as a ubiquitous neurotoxic mechanism of soluble amyloid oligomers. J Biol Chem 2005;280:17294–300.

[22] Furukawa K, Abe Y, Akaike N. Amyloid β protein-induced irreversible current in rat cortical neurones. Neuroreport 1994;5:2016–8.

[23] Hardy J, Selkoe DJ. The amyloid hypothesis of Alzheimer's disease: progress and problems on the road to therapeutics. Science 2002;297:353–6.

[24] Hertel C, Terzi E, Hauser N, Jakob-Rotne R, Seelig J, Kemp JA. Inhibition of the electrostatic interaction between β-amyloid peptide and membranes prevents beta-amyloid-induced toxicity. Proc Natl Acad Sci USA 1997;94:9412–6.

[25] Hirakura Y, Lin MC, Kagan BL. Alzheimer amyloid Ab1–42 channels: effects of solvent, pH, and congo red. J Neurosci Res 1999;57:458–66.

[26] Hope MJ, Cullis PR. Lipid asymmetry induced by transmembrane pH gradients in large unilamellar vesicles. J Biol Chem 1987;262:4360–6.

[27] Hope MJ, Redelmeier TE, Wong KF, Rodrigueza W, Cullis PR. Phospholipid asymmetry in large unilamellar vesicles induced by transmembrane pH gradients. Biochemistry 1989;28:4181–7.

[28] Jain MK, Wagner RF. Introduction to biological membranes. NY: Wiley, 1980.

[29] Ji SR, Wu Y, Sui SF. Cholesterol is an important factor affecting the membrane insertion of β-amyloid peptide (Ab1–40), which may potentially inhibit the fibril formation. J Biol Chem 2002;277:6273–9.

[30] Ji SR, Wu Y, Sui SF. Study of β-amyloid peptide (Ab40) insertion into phospholipid membranes using monolayer technique. Biochemistry (Moscow) 2002;67:1283–8.

[31] Kagan BL, Azimov R, Azimova R. Amyloid peptide channels. J Membr Biol 2004;202:1–10.

[32] Kagan BL, Hirakura Y, Azimov R, Azimova R, Lin MC. The channel hypothesis of Alzheimer's disease: current status. Peptides 2002;23:1311–5.

[33] Kawahara M. Disruption of calcium homeostasis in the pathogenesis of Alzheimer's disease and other conformational diseases. Curr Alzheimer Res 2004;1:87–95.

[34] Kawahara M, Arispe N, Kuroda Y, Rojas E. Alzheimer's disease amyloid β-protein forms Zn2+-sensitive, cation-selective channels across excised membrane patches from hypothalamic neurons. Biophys J 1997;73:67–75.

[35] Kawahara M, Kuroda Y, Arispe N, Rojas E. Alzheimer's β-amyloid, human islet amylin, and prion protein fragment evoke intracellular free calcium elevations by a common mechanism in a hypothalamic GnRH neuronal cell line. J Biol Chem 2000;275:14077–83.

[36] Kayed R, Sokolov Y, Edmonds B, McIntire TM, Milton SC, Hall JE, et al. Permeabilization of lipid bilayers is a common conformation-dependent activity of soluble amyloid oligomers in protein misfolding diseases. J Biol Chem 2004;279:46363–6.

[37] Kourie JI, Henry CL, Farrelly P. Diversity of amyloid β protein fragment [1–40]-formed channels. Cell Mol Neurobiol 2001;21:255–84.

[38] Kremer JJ, Sklansky DJ, Murphy RM. Profile of changes in lipid bilayer structure caused by β-amyloid peptide. Biochemistry 2001;40:8563–71.

[39] Kurganov B, Doh M, Arispe N. Aggregation of liposomes induced by the toxic peptides Alzheimer's Abs, human amylin and prion (106–126): facilitation by membrane-bound GM1 ganglioside. Peptides 2004;25:217–32.

[40] Lee G, Pollard HB, Arispe N. Annexin 5 and apolipoprotein E2 protect against Alzheimer's amyloid-β-peptide cytotoxicity by competitive inhibition at a common phosphatidylserine interaction site. Peptides 2002;23:1249–63.

[41] Lin H, Bhatia R, Lal R. Amyloid β protein forms ion channels: implications for Alzheimer's disease pathophysiology. FASEB J 2001;15:2433–44.

[42] Lin H, Zhu YJ, Lal R. Amyloid β protein (1–40) forms calcium-permeable Zn^{2+}-sensitive channel in reconstituted lipid vesicles. Biochemistry 1999;38:11189–96.

[43] Lin MC, Kagan BL. Electrophysiologic properties of channels induced by Ab25–35 in planar lipid bilayers. Peptides 2002;23:1215–28.

[44] Mattson MP, Cheng B, Davis D, Bryant K, Lieberburg I, Rydel RE. β-Amyloid peptides destabilize calcium homeostasis and render human cortical neurons vulnerable to excitotoxicity. J Neurosci 1992;12:376–89.

[45] McLaurin J, Chakrabartty A. Characterization of the interactions of Alzheimer β-amyloid peptides with phospholipid membranes. Eur J Biochem 1997;245:355–63.

[46] McLaurin J, Chakrabartty A. Membrane disruption by Alzheimer β-amyloid peptides mediated through specific binding to either phospholipids or gangliosides: implications for neurotoxicity. J Biol Chem 1996;271: 26482–9.

[47] Micelli S, Meleleo D, Picciarelli V, Gallucci E. Effect of sterols on β-amyloid peptide (AbP1–40) channel formation and their properties in planar lipid membranes. Biophys J 2004;86:2231–7.

[48] Michaelson DM, Horwitz AF, Klein MP. Head group modulation of membrane fluidity in sonicated phospholipid dispersions. Biochemistry 1974;13:2605–12.

[49] Mirzabekov TA, Lin MC, Kagan BL. Pore formation by the cytotoxic islet amyloid peptide amylin. J Biol Chem 1996;271:1988–92.

[50] Rhee SK, Quist AP, Lal R. Amyloid β protein-(1–42) forms calcium-permeable Zn^{2+}-sensitive channel. J Biol Chem 1998;273:13379–82.

[51] Sanderson KL, Butler L, Ingram VM. Aggregates of a β-amyloid peptide are required to induce calcium currents in neuron-like human teratocarcinoma cells: relation to Alzheimer's disease. Brain Res 1997;744:7–14.

[52] Sponne I, Fifre A, Koziel V, Oster T, Olivier JL, Pillot T. Membrane cholesterol interferes with neuronal apoptosis induced by soluble oligomers but not fibrils of amyloid-β peptide. FASEB J 2004;18:836–8.

[53] Terzi E, Holzemann G, Seelig J. Interaction of Alzheimer β-amyloid peptide(1–40) with lipid membranes. Biochemistry 1997;36:14845–52.

[54] Vargas J, Alarcon JM, Rojas E. Displacement currents associated with the insertion of Alzheimer disease amyloid β-peptide into planar bilayer membranes. Biophys J 2000;79:934–44.

[55] Weiss JH, Pike CJ, Cotman CW. Ca^{2+} channel blockers attenuate β-amyloid peptide toxicity to cortical neurons in culture. J Neurochem 1994;62:372–5.

[56] Woolley GA, Deber CM. A lipid vesicle system for probing voltage-dependent peptide–lipid interactions: application to alamethicin channel formation. Biopolymers 1989;28:267–72.

[57] Yip CM, Elton EA, Darabie AA, Morrison MR, McLaurin J. Cholesterol: a modulator of membrane-associated Ab-fibrillogenesis and neurotoxicity. J Mol Biol 2001;311: 723–34.

[58] Zhao H, Tuominen EK, Kinnunen PK. Formation of amyloid fibers triggered by phosphatidylserine-containing membranes. Biochemistry 2004;43:10302–7.

[59] Zhou Y, Richardson JS. Cholesterol protects PC12 cells from β-amyloid induced calcium disordering and cytotoxicity. Neuroreport 1996;7:2487–90.

[60] Zhu YJ, Lin H, Lal R. Fresh and nonfibrillar amyloid β protein(1–40) induces rapid cellular degeneration in aged human fibroblasts: evidence for AbP-channel-mediated cellular toxicity. FASEB J 2000;14:1244–54.